JACS
JOURNAL OF THE AMERICAN CHEMICAL SOCIETY
Article
pubs.acs.org/JACS

BLUF Domain Function Does Not Require a Metastable Radical Intermediate State

Andras Lukacs,[§,#] Richard Brust,[‡,⊥] Allison Haigney,[‡,†] Sergey P. Laptenok,[§] Kiri Addison,[§] Agnieszka Gil,[‡] Michael Towrie,[∥] Gregory M. Greetham,[∥] Peter J. Tonge,*[,‡] and Stephen R. Meech*[,§]

[‡]Department of Chemistry, Stony Brook University, Stony Brook, New York 11794-3400, United States
[§]School of Chemistry, University of East Anglia, Norwich NR4 7TJ, U.K.
[∥]Central Laser Facility, Research Complex at Harwell, Harwell Science and Innovation Campus, Didcot, Oxon OX11 0QX, U.K.
[#]Department of Biophysics, Medical School, Szigeti Strasse 12, H-7624 Pécs, Hungary

Supporting Information

ABSTRACT: BLUF (blue light using flavin) domain proteins are an important family of blue light-sensing proteins which control a wide variety of functions in cells. The primary light-activated step in the BLUF domain is not yet established. A number of experimental and theoretical studies points to a role for photoinduced electron transfer (PET) between a highly conserved tyrosine and the flavin chromophore to form a radical intermediate state. Here we investigate the role of PET in three different BLUF proteins, using ultrafast broadband transient infrared spectroscopy. We characterize and identify infrared active marker modes for excited and ground state species and use them to record photochemical dynamics in the proteins. We also generate mutants which unambiguously show PET and, through isotope labeling of the protein and the chromophore, are able to assign modes characteristic of both flavin and protein radical states. We find that these radical intermediates are not observed in two of the three BLUF domains studied, casting doubt on the importance of the formation of a population of radical intermediates in the BLUF photocycle. Further, unnatural amino acid mutagenesis is used to replace the conserved tyrosine with fluorotyrosines, thus modifying the driving force for the proposed electron transfer reaction; the rate changes observed are also not consistent with a PET mechanism. Thus, while intermediates of PET reactions can be observed in BLUF proteins they are not correlated with photoactivity, suggesting that radical intermediates are not central to their operation. Alternative nonradical pathways including a keto−enol tautomerization induced by electronic excitation of the flavin ring are considered.

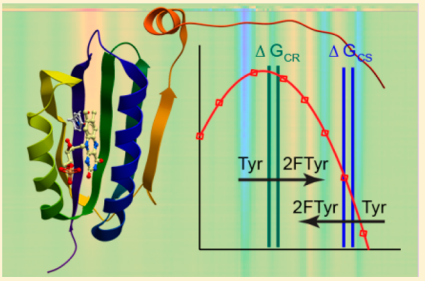

INTRODUCTION

Light-sensing proteins mediate the response of living systems to light. In the most widely studied examples, rhodopsins, phytochromes, and photoactive yellow protein, the primary process involves an excited state isomerization reaction.[1,2] Relatively recently a range of blue-light-sensing flavoproteins have been discovered and shown to be widespread, occurring in animals, plants, fungi, and bacteria.[3−5] Three separate classes have now been identified: photolyase/cryptochromes; light-oxygen-voltage (LOV) domain proteins; blue light sensing using FAD (BLUF) domain proteins. In each case the chromophore is a flavin (isoalloxazine) ring which is planar in its oxidized form and thus not able to exert a mechanical force on the surrounding protein. Consequently the mechanism of operation of these photoactive flavoproteins is a topic of intense experimental and theoretical investigation.[6,7] In the DNA repair enzyme, photolyase, a change in oxidation state of the flavin is observed, while in the LOV domain a reaction of the triplet state of the flavin with an adjacent cysteine is the primary mechanism.[8−11]

The BLUF domain is a versatile unit involved in phototaxis in *Synechocystis*,[12,13] biofilm formation in *Acinetobacter baumannii*,[14] and gene expression in *Rhodobacter sphaeroides*,[15,16] processes which are controlled by the BLUF proteins PixD (Slr1694) and BlsA and activation of photopigment and PUC A protein (AppA), respectively. In addition to this importance in nature some applications for flavoproteins have been proposed. For example, the role of the BLUF domain in light-induced regulation of gene expression makes it a candidate for exploitation in the emerging field of optogenetics,[17] while the use of photoactive flavoproteins as sources of genetically expressed singlet oxygen has been proposed.[18,19] Despite this interest and importance, the primary mechanism operating in the BLUF domain is as yet unresolved, and forms the topic of the present paper.

Conversion of the dark-adapted state of BLUF proteins to the signaling state under blue (∼450 nm) light leads to a red-shift in the ground state absorption of the flavin ring by 10−15 nm, with the flavin remaining in its fully oxidized form in both states.[20,21] The light-adapted state thus formed relaxes back to the dark state in the absence of irradiation in a time which is

Received: November 27, 2013
Published: March 2, 2014

   dx.doi.org/10.1021/ja4121082 | J. Am. Chem. Soc. 2014, 136, 4605−4615

dependent on the particular BLUF domain protein: 30 min for AppA, 9 min in BlsA, but much faster (<10 s) in PixD.

AppA is the best characterized of all BLUF domain proteins.[22−24] In the photosynthetic organism it acts as an antirepressor, responsible for light-activated control of the expression of genes involved in the biosynthesis of the photosynthetic apparatus. It comprises an N-terminal BLUF domain and a C-terminal domain which binds the repressor molecule PpsR in the dark. Irradiation with blue light causes dissociation of the AppA:PpsR complex. The structure of the BLUF domain ($AppA_{BLUF}$) has been studied by X-ray, NMR, and QM/MM and purely classical calculations.[22,23,25−31] An X-ray structure is shown in Figure 1, and the existence of an

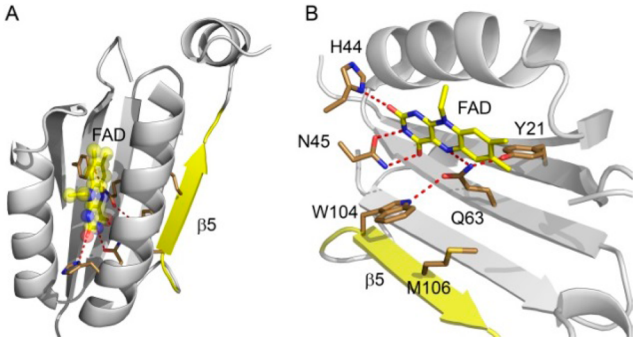

Figure 1. Structure and H-bonding of flavin adenosine dinucleotide (FAD) in $AppA_{BLUF}$. (A) Crystal structure of $AppA_{BLUF}$ showing flavin binding between helices 1 and 2; (B) the hydrogen bonding network around the flavin that includes the key residues Y21, Q63, W104, and M106. The figure was made using Pymol[36] and the structure 1YRX.pdb.[22]

intricate H-bonding network involving the flavin ring and residues Y21, Q63, W104, and M106 is apparent. Currently, X-ray structures disagree on the orientation of Q63 and W104, but both NMR and QM/MM calculations suggest that Q63 is mobile and flips between light and dark states, leading to modified H-bonded interactions between Q63, Y21, and the flavin ring.[25,32,33] A change in H-bonding between protein and the flavin on light activation (Figure 1) is supported by light minus dark IR difference measurements and Raman spectroscopy, where a red-shift is observed in the transition associated with the C4═O stretch mode of the flavin ring.[21,34,35]

In agreement with the structure and spectroscopy, site-directed mutagenesis shows that the residues Y21 and Q63 are essential for the light-activated function.[37,38] When these residues are mutated, the red-shift in the flavin absorption characteristic of a photoactive state is not observed. On the other hand W104 can be exchanged in AppA, and the red-shift is retained, but the light-to-dark recovery rate is dramatically enhanced (for example when Trp is replaced by Ala there is an 80-fold increase in the recovery rate), and biological activity is abolished.[39] We have shown elsewhere in femtosecond to millisecond IR spectroscopy that this mutation shortcircuits the structure change in AppA, thereby abolishing *in vivo* activity.[40]

The originally proposed and most widely accepted model for the primary process in BLUF domains is electron transfer from a highly conserved tyrosine residue (Y21 in AppA) to the photoexcited flavin ring, $Y21-FAD^* \rightarrow Y21^{\bullet+}-FAD^{\bullet-}$. This assignment is based on two important observations: the formation of a radical like spectrum in ultrafast transient electronic spectroscopy of PixD and the observation of complex multiexponential kinetics in the decay of the transient electronic spectrum.[38,41−46] Such multiexponential kinetics could be consistent with sequential formation of $FAD^{\bullet-}$ and $FADH^{\bullet}$ on a subnanosecond time scale.[45] However, in AppA no radical state was observed either by ultrafast electronic or transient infrared spectroscopy.[47,48] The electron transfer reaction was inferred by analogy with the PixD result and through analysis of the complex kinetics, which persist in AppA. An alternative proposal was presented, based on transient IR spectroscopy of AppA and its mutants, that photoexcitation of the flavin ring initiates a prompt change in the H-bonding environment without a change in oxidation state, which is sufficient to initiate structural change through a tautomerization in the Q63 residue.[48,49] Quite recently two other BLUF domain proteins (BlsA and BlrB) were investigated by ultrafast electronic and vibrational spectroscopy, respectively; again, no radical spectrum was detected, although complex kinetics were observed.[50,51] These results raise the key question of whether formation of a radical intermediate is critical to the operation of the BLUF domain. For example, a number of recent theoretical approaches to modeling the mechanism of signaling state formation in BLUF proteins assume formation of an electron transfer intermediate.[26,52−54]

Here we resolve this question by studying three dark-adapted BLUF domains, $AppA_{BLUF}$, PixD, and BlsA with 100 fs temporal resolution transient infrared (TRIR) spectroscopy with 4 cm^{-1} spectral resolution. These data are compared with TRIR of $AppA_{BLUF}$ mutants and model flavins which unambiguously display the spectra of radical intermediates.[55−57]

In this way marker bands for neutral and radical states are identified. These assignments are confirmed by isotope substitution. We then track the presence or absence of radical states in the three BLUF domains in their dark-adapted states. Finally, to further probe the role of photoinduced electron transfer we modulate the redox potential of the tyrosine residue in $AppA_{BLUF}$, suggested to act as the electron donor,[45,54] using unnatural amino acid substitution.[58] This comprehensive study allows us to describe the role of radical intermediate states in the BLUF photocycle. Such intermediates are observed in a number of proteins, but their presence is not correlated with photoactivity. Thus, an alternative mechanism for BLUF domain function is proposed.

EXPERIMENTAL METHODS

Transient Spectroscopy. The transient infrared spectrometer is based on the ULTRA apparatus described in detail elsewhere[59] with additional details given in the Supporting Information (SI). Key features are the stability and 10 kHz repetition rate which permit the acquisition of transient IR difference (TRIR) spectra with 100 fs time resolution and a signal-to-noise which allow the detection of transient changes in optical density as small as 10 μOD. Such high signal-to-noise supports detailed global analysis procedures described in the SI.

Materials and Protein Preparation. Methods for the preparation of AppA, the uniformly ^{13}C-labeled AppA and the AppA mutants have been presented elsewhere.[49] Additional details are provided in SI. Synthesis of 2-fluorotyrosine (2-FTyr) and 3-fluorotyrosine (3-FTyr) was performed as described by Stubbe,[60,61] and additional details are provided in SI.

Redox Potentials. The formal potentials at physiological pH of Tyr, 2-FTyr, and 3- FTyr were recorded using an Autolab PGStat302N computer-controlled potentiostat (Metrohm) in pH 7.0 phosphate buffer using square wave voltammetry. A three-electrode cell was used comprising a 3 mm glassy carbon working electrode, a Pt counter electrode (99.99% Goodfellow), and a saturated calomel reference electrode (Radiometer). The applied potential was modulated in

dx.doi.org/10.1021/ja4121082 | J. Am. Chem. Soc. 2014, 136, 4605−4615

square-waveform with the following parameters: pulse amplitude 25 mV, frequency 12.5 Hz, step potential 2 mV. Scanning in an oxidative direction revealed a single oxidation peak for each amino acid derivative. The oxidation of the amine moiety in each species is electrochemically irreversible, therefore the formal potential is found simply by subtracting the pulse amplitude from the observed peak potential.[62] Note that, as the oxidation process involves concomitant proton and electron transfer, at physiological pH the formal potentials used herein differ from standard potential literature values (which by definition refer to the standard potential at pH 1.0) by ∼−55 mV/pH unit. Data analysis was performed using the on-board potentiostat software Nova v 1.10.

RESULTS AND DISCUSSION

Transient IR Spectroscopy of AppA. Figure 2A shows the experimentally measured TRIR difference spectra for the dark-adapted state of the AppA BLUF domain ($dAppA_{BLUF}$) evolving between 1 ps and 1 ns after excitation at 450 nm. These are similar to spectra presented earlier,[48] but experimental developments yield spectra with greatly improved signal-to-noise over a wider spectral range, which encompasses a number of newly observed modes. From a comparison with the TRIR of FMN in buffer solution (Figure 2B) it is evident that on the nanosecond time scale the $dAppA_{BLUF}$ spectrum is dominated by flavin ring localized vibrational modes, with negative (bleach) peaks arising from depletion of the electronic ground state and positive peaks appearing during the excitation pulse arising from excited state modes. Detailed assignments based on DFT calculations and isotopic substitutions have been presented elsewhere.[55,56,63−65] Essentially the two highest-frequency bleach modes (1701 and 1653 cm^{-1}) arise from a coupled pair of carbonyl stretch/N3H wag modes, while the narrow bleaches at 1584 (weak) and 1548 cm^{-1} (strong) are flavin ring modes. The complex line shape between 1600 and 1653 cm^{-1} contains contributions from both the excited electronic state of the flavin ring and protein modes perturbed by electronic excitation. The assignment of modes to the protein has been confirmed by studies of the fully ^{13}C-labeled dAppA (SI, Figure S1) and described elsewhere.[49] An important result in Figure 2A is the observation of a pair of broad transient absorptions at 1380 and 1415 cm^{-1}. These are assigned to the singlet excited state of the flavin ring, because they are clearly also present in the TRIR of FMN in solution[65] (Figure 2B). Thus, the 1380 cm^{-1} transient and intense 1548 cm^{-1} bleach intensities can be taken as marker modes, indicating the population of the excited state and ground state, respectively, of FAD in $dAppA_{BLUF}$. In line with this assignment these bands appear within the excitation pulse, and their temporal evolution is simply a decrease in amplitude without any spectral shift (Figure 2C).

The temporal evolution of the spectra in Figure 2A is in other respects rather featureless; despite the marked improvement in signal-to-noise compared to earlier data, there is no evidence for the formation of intermediate species with distinct vibrational spectra on the subnanosecond time scale. Essentially the spectra in Figure 2A appear within the excitation pulse and mainly relax back to the electronic ground state. In contrast to this relatively simple spectroscopy the relaxation kinetics are complex and can only be fit with a sum of at least two exponential decay terms (Table 1). This should not be taken as necessarily indicating two distinct states, but rather a minimum numerical representation of multiexponential kinetics. Such complex kinetics may indicate an inhomogeneous ground state distribution, with different decay kinetics for different

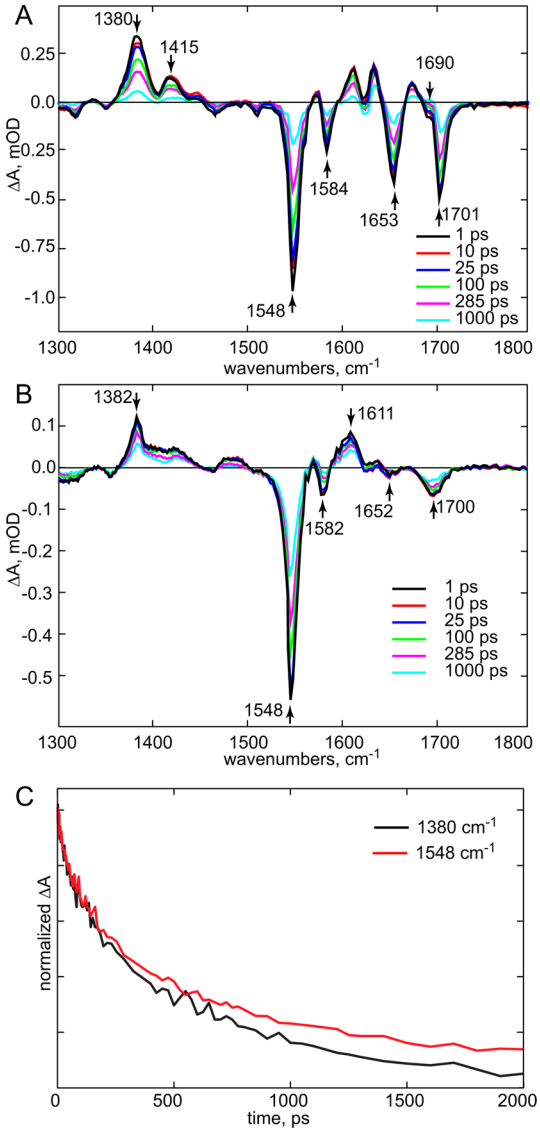

Figure 2. Comparison of TRIR for $dAppA_{BLUF}$ and FMN. (A) Temporal evolution of TRIR spectra of $dAppA_{BLUF}$. (B) Temporal evolution of the TRIR spectra of FMN in aqueous buffer. (C) Comparison of the excited state decay (1380 cm^{-1}) and ground state recovery (1548 cm^{-1}) dynamics of $dAppA_{BLUF}$. The 1548 cm^{-1} data have been inverted and normalized for the comparison. The difference at long time reflects the fact that the excited singlet state relaxes completely but the ground state is not completely repopulated due to population of long-lived state; this is modeled by a constant offset for the analysis in Table 1.

conformations of the protein around the flavin ring. In at least one case (the 1690 cm^{-1} shoulder on the 1701 cm^{-1} bleach, Figure 2A) spectrally distinct states are observed to have different ground state recovery lifetimes. The faster recovery of the 1690 cm^{-1} bleach is particularly noteworthy because it correlates with the faster ground state recovery of the light-adapted state ($lAppA_{BLUF}$), which has a red-shifted C4═O carbonyl mode (see SI Figure S2). This may indicate the existence of a fraction of the light state structure even in the dark-adapted protein.

In Figure 2C the kinetics associated with the flavin ring ground and excited state marker modes of $dAppA_{BLUF}$ at 1380 and 1548 cm^{-1} are compared. The kinetics are of opposite sign but otherwise cannot be distinguished from one another, aside

dx.doi.org/10.1021/ja4121082 | J. Am. Chem. Soc. 2014, 136, 4605−4615

Table 1. Excited State Decay and Ground State Recovery Kinetics at the Two Characteristic Frequencies for Dark-Adapted BLUF Domains and Mutants Y21W and Y8W[a]

BLUF	frequency/cm^{-1}	wt τ_1	τ_1/ps	τ_2/ps
dAppA	1380	0.38	17 ± 8	401 ± 110
	1548	0.42	29 ± 5	512 ± 60
Y21W	1380	0.59	5 ± 1	85 ± 9
	1548	0.57	49 ± 11	168 ± 50
PixD	1380	0.48	15 ± 4	154 ± 29
	1548	0.47	28 ± 4	226 ± 28
Y8W	1380	0.75	2 ± 0.5	42 ±15
	1548	0.60	11 ± 2	108 ± 19
BlsA	1380	0.37	11 ± 3	397 ± 70
	1548	0.44	12 ± 3	375 ± 60

[a]Kinetics were fit to a sum of two exponential terms, with the time constants τ_i and normalized weights (wt τ_i + wt τ_2 = 1). An additional offset is included to account for incomplete recovery of the 1548 cm^{-1} ground state.

from the constant offset in the ground state recovery (1548 cm^{-1}), which is associated with microsecond relaxation dynamics.[40] This offset is also evident in independent global analysis (Figure S3 in SI). The corresponding two exponential fits are the same within the fitting error (Table 1). Such close agreement of excited state decay and ground state recovery is inconsistent with a sequential kinetics model in which the excited state is quenched to form a distinct intermediate state which then relaxes on a longer time scale to form the light-adapted state. In that case the 1380 cm^{-1} excited state transient would relax faster than the 1548 cm^{-1} ground state recovers. Thus, there is no evidence in these data for the existence of distinct intermediates in the subnanosecond kinetics of dAppA$_{BLUF}$. That the dynamics are nonsingle exponential most likely reflects a distribution of ground state structures in the protein (for which there is some evidence in Figure 2A and some calculations[33]).

The quality of the data in Figure 2A is sufficient to conduct a global kinetic analysis. To make meaningful comparisons between all samples studied (see below) we restricted modeling to two simple cases, first the construction of decay-associated spectra (DAS) with two decaying and one nondecaying (final) state and second evolution-associated spectra (EAS) using a single intermediate scheme, A→B→C. Both schemes fit the data adequately and equally well. Thus, to distinguish between them it is critical to have additional criteria, in particular a distinct spectrum that can be associated with any intermediate state. More complex models with additional intermediates or decaying states yield a slight improvement in the quality of the fit, but no new physical insight. The results are shown in SI (Figure S3). The DAS show minor 30 ps and major 485 ps decaying components plus a final spectrum. This aligns closely with the biexponential kinetics of the marker modes (Table 1, Figure 2C); it is significant that the 30 ps DAS is similar to the transient spectrum of lAppA$_{BLUF}$ (Figure S2 in SI). For the EAS the initial and intermediate states have essentially the same spectra. Thus, global analysis also does not support the formation of an intermediate state. Both models yield essentially the same 'final' spectrum, and its microsecond kinetics (responsible for the offset in Figure 2C) have been described elsewhere.[40]

To summarize, for dAppA$_{BLUF}$ no bands are found in the TRIR spectra which can be assigned specifically to formation of a radical (or any other) intermediate state in the photocycle. Further, the kinetics do not point to population of a distinct intermediate state. There is evidence for an inhomogeneous ground state distribution giving rise to complex kinetics, which may include structures similar to the light-activated state, lAppA$_{BLUF}$.

Observation of Radical States in dAppA$_{BLUF}$ Mutants. To investigate the role of radical states in the primary photochemistry of dAppA$_{BLUF}$ the Y21W mutant was studied by TRIR and transient absorption. This protein is photoinactive,[39] with no red shift in the spectrum of the dark-adapted state on irradiation. However, electron transfer quenching of the flavin excited state is expected to be significantly faster in Y21W than in dAppA$_{BLUF}$ because the driving force for charge separation is larger (more negative) by ∼300 mV when Tyr is replaced by Trp.[66] It was reported by Bonetti et al.[38] that the equivalent Y8W substitution in PixD opened up a new radical pathway, W8−FAD → W8$^{\bullet+}$−FAD$^{\bullet-}$ (in PixD the Y8−FAD → Y8$^{\bullet+}$−FAD$^{\bullet-}$ radical absent in dAppA$_{BLUF}$ is observed;[45] see also section 3.3). Analysis of TRIR data for Y21W will require marker modes for possible radical states. We have previously reported vibrational mode assignments for FAD$^{\bullet-}$ and FADH$^{\bullet}$ ground states, and assigned transitions at 1528 cm^{-1} and 1626 cm^{-1} to the ground state of the radical (radical spectra are presented in SI Figure S4).[64] These radical marker modes complement those identified above for the neutral reactants. Although the 1626 cm^{-1} region in dAppA$_{BLUF}$ is crowded due to contributions from both protein and flavin, the 1528 cm^{-1} region is not and does not show the growth of an absorption which could be assigned to formation of FAD$^{\bullet-}$ (Figure 2A); thus, there is no positive evidence for a radical state in the wild-type protein.

The TRIR spectra for Y21W dAppA$_{BLUF}$ are shown in Figure 3A. That a new reaction pathway has been introduced is immediately apparent from the spectra (Figure 3A) and kinetics (Figure 3B). There are transient absorptions at 1521 and 1637 cm^{-1} that are absent in wild-type dAppA$_{BLUF}$. Both peaks show true intermediate kinetics, increasing in amplitude as a function of time after excitation, reaching a maximum at around 10 ps, and decaying on a slower time scale (Figure 3B). The 1521 cm^{-1} transient is assigned to formation of a flavin radical by photoexcited electron transfer from Trp21, while the intense 1637 cm^{-1} peak may have contributions from FAD$^{\bullet-}$ and/or the Trp$^{\bullet+}$ radical cation.

Along with the formation of these new transient states, a time-dependent bleach is expected, as some ground state species must be consumed in the reaction. Such consumption kinetics are seen in the increasingly negative bleach at 1626 cm^{-1} (Figure 3A). Thus, the spectra and kinetics of Y21W are consistent with a sequential electron transfer reaction, W21−FAD* → W21$^{\bullet+}$−FAD$^{\bullet-}$ → W21−FAD The sequential nature of the kinetics is supported by comparison of the FAD* decay (1380 cm^{-1}) which should reflect the primary electron transfer rate, and FAD ground state recovery (1548 cm^{-1}), which will also depend on the rate of charge recombination (Table 1, Figure 3C). The FAD excited state decays more rapidly than the ground state recovers, in line with the formation of an intermediate state but in contrast to the behavior of dAppA$_{BLUF}$ (Figure 2C, Table 1). As for wild-type dAppA$_{BLUF}$ the kinetics of Y21W are nonsingle exponential (Table 1) even for the decay of FAD*. This again probably reflects a distribution of ground state structures in Y21W.

dx.doi.org/10.1021/ja4121082 | J. Am. Chem. Soc. 2014, 136, 4605−4615

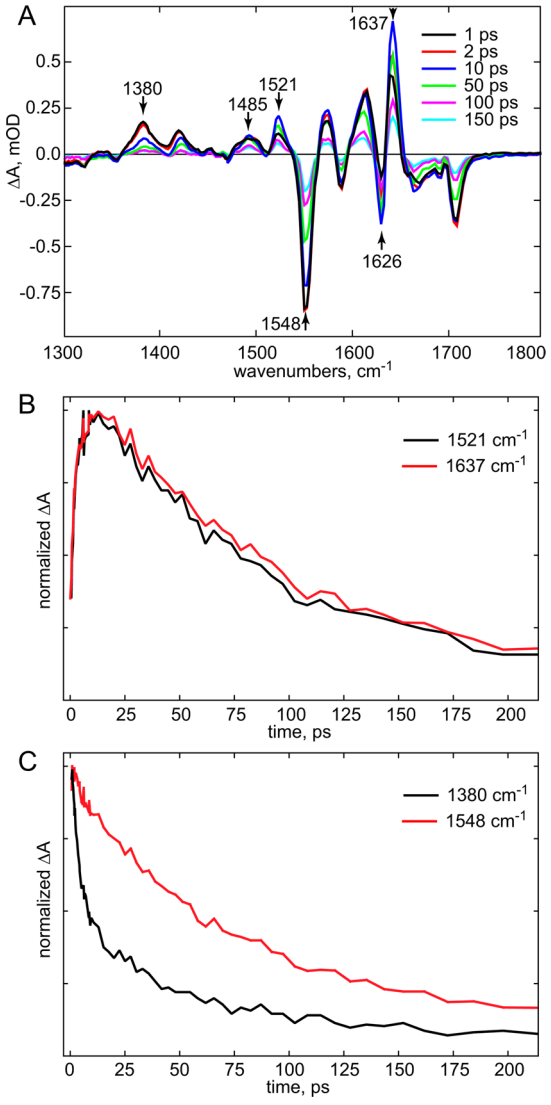

Figure 3. TRIR of Y21W. (A) Temporal evolution of TRIR spectra. (B) Rise and decay kinetics associated with radical product states at 1521 cm^{-1} and 1637 cm^{-1}. (C) Excited state decay (black) and ground state recovery (red) kinetics.

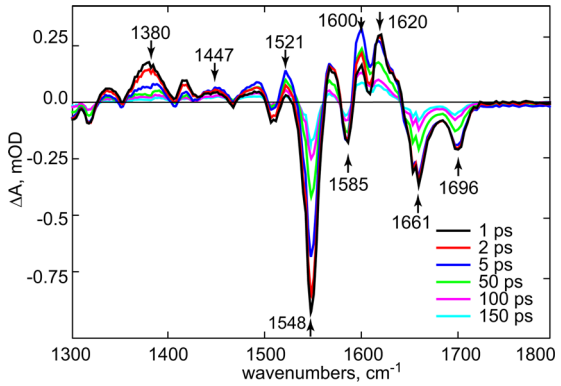

Figure 4. TRIR of $U^{13}C$–Y21W . The bands assigned to the flavin and to its radical anion are unaffected by the isotope exchange, while those of the electron donor, Trp21, shift relative to those in Figure 3

Further proof that an electron transfer reaction occurs in Y21W was obtained from transient visible absorption spectroscopy (SI Figure S5) In that case the Trp radical cation spectrum of Y21W is shown to rise and decay with the same kinetics as the 1640 cm^{-1} mode.

To confirm these assignments of protein and flavin modes in the TRIR spectra of Y21W, the fully ^{13}C-labeled protein $U^{13}C$–Y21W was studied (Figure 4). As expected, the main bleach modes associated with the flavin ring (1548, 1585 cm^{-1}) occur at essentially the same frequency as in $dAppA_{BLUF}$, although the highest-frequency carbonyl bleach unexpectedly shifts down from 1701 to 1696 cm^{-1}. This shift suggests a contribution from an instantaneous bleach of a protein mode underlying the C4═O flavin bleach in Y21W. At this frequency the most probable assignment of the protein bleach is to a change in either oscillator strength or frequency of a carbonyl mode in an amino acid side chain H-bonded to the flavin. Such instantaneous bleach modes were previously reported in the photoinactive mutant Q63E.[49] The ^{13}C substitution leads to major changes in the 1580–1680 cm^{-1} region, with the intense transient peak at 1637 cm^{-1} shifting to 1600 cm^{-1} and the associated bleach shifting from 1626 cm^{-1} to become a minimum at 1585 cm^{-1} (strongly overlapped with the flavin ring mode). The downshift of this pair on isotopic substitution confirms that they arise from vibrational modes of the electron donor, the W21 residue; thus both donor and acceptor states are observed simultaneously by TRIR. Unfortunately, there is only limited data on the IR spectra of Trp radicals or the radical cation, making further assignment to specific vibrational modes difficult.[67] The final major effect of ^{13}C exchange is an increase in the amplitude of the 1661 cm^{-1} bleach compared to that of Y21W. This bleach is assigned in $dAppA_{BLUF}$ to the lower-frequency flavin carbonyl mode, C2═O,[55,56] and the apparently stronger bleach in fact arises from the downshift of the absorption of the radical product mode which partially obscures this transient in Y21W.

Importantly, the transient species growing in at 1521 cm^{-1} does not shift on ^{13}C labeling, consistent with its assignment to formation of the flavin radical anion on the picosecond time scale (Figure 4). The absence of this feature from the spectra of wild-type $dAppA_{BLUF}$ (Figure 2A) therefore argues against significant population of the flavin radical intermediate state in the AppA photocycle. The spectral region from 1500 cm^{-1} down to 1430 cm^{-1} has only one weak bleach feature in $dAppA_{BLUF}$ (Figure 2A) but in Y21W (Figure 3A) a new transient absorption grows in at 1485 cm^{-1} with the same kinetics as the flavin radical at 1521 cm^{-1}. In $U^{13}C$–Y21W an additional transient feature rises at 1447 cm^{-1} and decays (Figures 3A,4). The 1485 cm^{-1} mode in Y21W is unshifted on ^{13}C substitution, and thus, is assigned to the flavin radical (which aligns with a feature seen in the glucose oxidase radical spectrum[64]). The 1447 cm^{-1} transient which appears only in $U^{13}C$–Y21W must arise from a mode of the Trp radical cation, shifted down from a position underlying the 1480–1520 cm^{-1} region in the Y21W.

The observation of a clear rising component in the TRIR data invites application of the sequential kinetic model in global analysis; the resulting EAS for Y21W and $U^{13}C$–Y21W are shown in Figure 5. The spectra correlate with the discussion of the raw data above and add some new details. The band at 1701 cm^{-1} shifts, weakens, and broadens on ^{13}C substitution, showing that the protein bleach mode underlying the C4═O carbonyl has shifted down to fill in the feature at 1690 cm^{-1}. As discussed above, this is associated with a carbonyl mode in a protein residue, instantaneously perturbed on excitation of the

dx.doi.org/10.1021/ja4121082 | J. Am. Chem. Soc. 2014, 136, 4605–4615

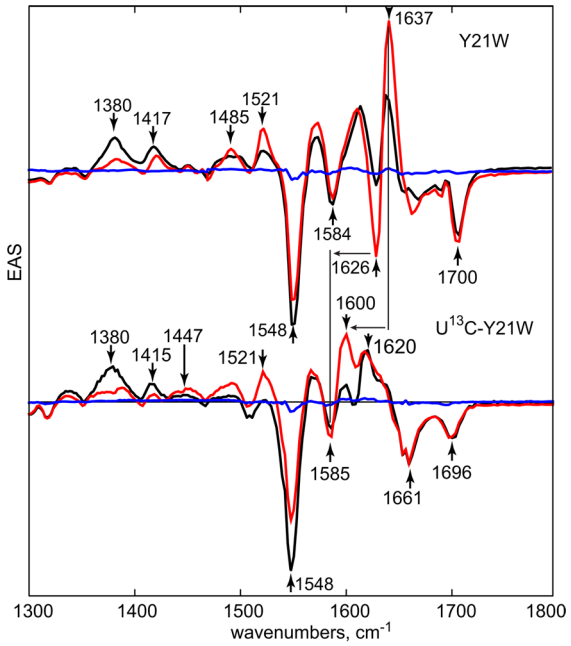

Figure 5. Evolution-associated spectra for Y21W and $U^{13}C$–Y21W. The kinetic scheme is A→B→C, and the sequence of the EAS is black→red→blue.

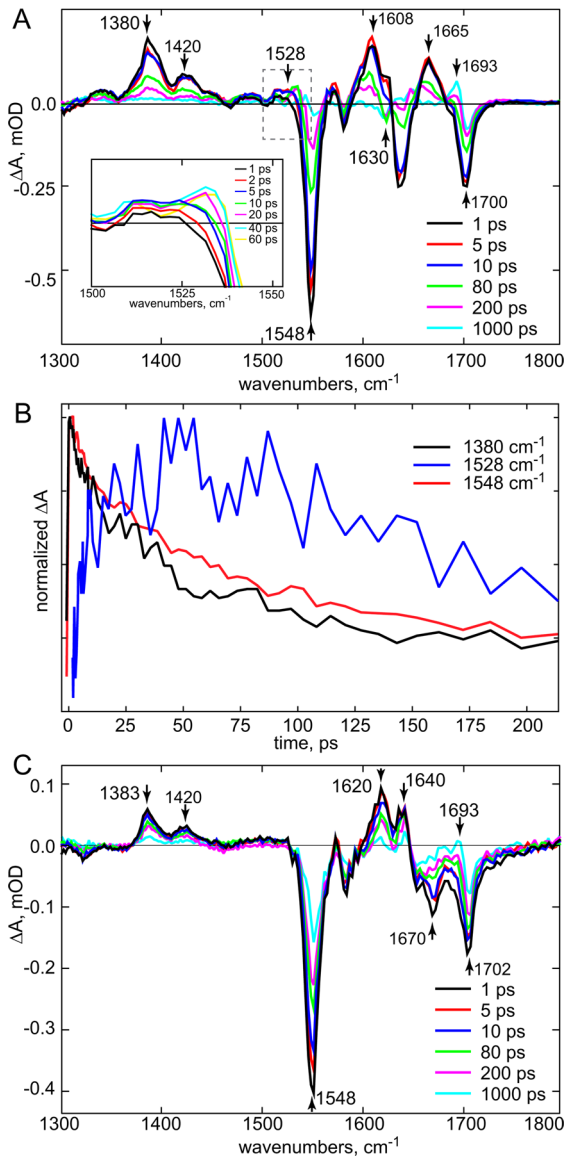

Figure 6. TRIR of BLUF domain proteins. (A) Temporal evolution of TRIR for PixD. (B) PixD transient kinetics at excited state, radical intermediate (1528 cm^{-1}) and ground state modes. (C) Temporal evolution of TRIR for BlsA.

flavin ring. Further assignment will require specific isotope editing of residues H-bonded to the flavin. The intense pair of modes assigned to the Trp → $Trp^{\bullet+}$ reaction are downshifted by isotope substitution, as expected. In $U^{13}C$–Y21W this pair is overlapped with features at ~1610 and 1580 cm^{-1} which do not themselves shift on isotopic exchange and can thus be assigned as flavin modes. In addition to the previously noted rising feature of $FAD^{\bullet-}$ at 1521 cm^{-1} (which does not shift on isotope exchange) new features associated with the radical intermediate are also resolved in the global analysis at 1485 cm^{-1} ($FAD^{\bullet-}$) and 1447 ($Trp^{\bullet+}$). Finally it is significant that the final EAS for Y21W and $U^{13}C$–Y21W (Figure 5) are very close to the baseline. The long-lived perturbation to the protein structure seen in $dAppA_{BLUF}$ is absent in Y21W, consistent with the latter being a photoinactive protein.

Thus, these data on Y21W show that photoinduced electron transfer reactions can be observed in BLUF domain proteins by TRIR and that there are a number of characteristic marker bands for radical intermediates states of both electron donor and acceptor. The absence of these modes from the $dAppA_{BLUF}$ spectrum argues against the formation of a significant population of radical intermediate states during its photocycle.

TRIR of BLUF Domains PixD and BlsA. In Figure 6 the evolution of the TRIR spectra for two further BLUF domain proteins, PixD and BlsA, are shown. The ultrafast dynamics of PixD have been studied in detail by Kennis and co-workers through transient electronic spectroscopy.[38,45] They observed radical states in PixD. The photocycle of the recently characterized BlsA BLUF protein has been described by us.[50] Comparison of the TRIR spectra immediately shows distinct differences between them (Figure 6).

The most remarkable observation is the clear growth of the flavin radical in PixD on the tens of picoseconds time scale at 1528 cm^{-1} (Figure 6A). In contrast to PixD, but in common with $dAppA_{BLUF}$ (Figure 2A), no such radical state is observed for BlsA (Figure 6C). The results of the biexponential analysis of PixD at 1380 and 1548 cm^{-1} marker modes are included in Table 1. As expected for a sequential electron transfer reaction, the excited state decays more rapidly than the ground state is repopulated, although the difference is not as large as in Y21W $AppA_{BLUF}$, consistent with the larger driving force in the latter. For BlsA the same marker modes show no difference in the excited state decay and ground state recovery kinetics, as was also found for $dAppA_{BLUF}$ (Table 1, Figure 2C). A further significant difference is that PixD has overall faster kinetics than BlsA and $dAppA_{BLUF}$, as already noted by Gauden et al.[45] Thus, these observations confirm not only the importance of the electron transfer reaction in PixD but also that the observation of radical intermediate states is the exception rather than the rule for the four BLUF domains studied by ultrafast spectroscopy (BlrB also did not show the radical transient[51]). Evidently different BLUF domains exhibit different excited state chemistry.

dx.doi.org/10.1021/ja4121082 | J. Am. Chem. Soc. 2014, 136, 4605–4615

An important question is the identity of the electron donor in PixD, usually assumed to be the adjacent tyrosine, Y8. No modes are observed in Figure 6A which can be clearly associated with a radical cation (a bleach does develop at 1630 cm^{-1}, but this is not sufficient to assign the electron donor to Y8 as the flavin ring has modes in this range). To compare with Y21W the corresponding Y8W mutant of PixD was prepared. The effect of mutation is to dramatically accelerate the quenching of FAD* and also to increase the rate of ground state recovery (Table 1). The EAS recovered for the TRIR data for PixD (Figure 6A) and Y8W (SI Figure S6) are shown in Figure 7. Again, the most striking feature is the appearance in

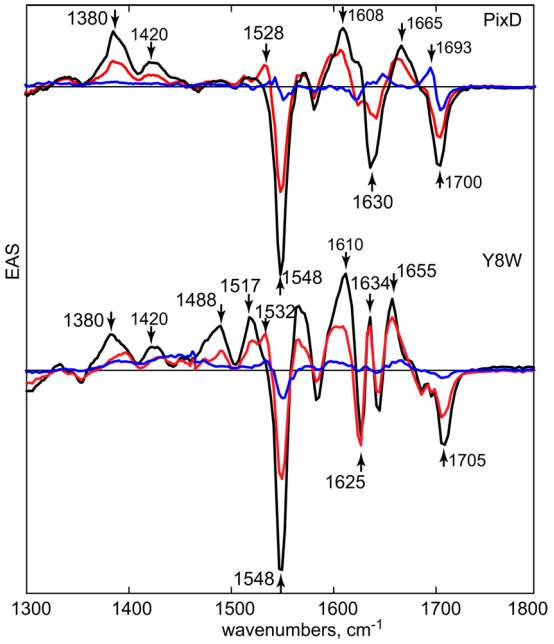

Figure 7. Evolution-associated spectra for PixD and Y8W PixD. The kinetic scheme is A→B→C and the sequence of the EAS is black→red→blue.

Y8W of the differential line shape 1625/1634 cm^{-1}, obscuring the lower-frequency carbonyl bleach of the flavin ring. This agrees closely with observations in the Y21W $AppA_{BLUF}$ (Figure 3a, 5), consistent with a Trp electron donor. However, no strong rise time is associated with this pair in Y8W, which we ascribe to the fact that the electron transfer reaction is too fast (Table 1) for the rise to be resolved from the multiple contributions to the signal at this wavenumber. The absence of this characteristic pair of modes in PixD is therefore consistent with a Tyr electron donor rather than the more remote W91 residue, which also aligns with the considerably slower overall kinetics compared with those of Y8W. Finally the different final EAS for PixD and Y8W, with only the former showing residual features at 1700 and 1625 cm^{-1}, indicate a long-lived perturbation of the protein structure characteristic of the photoactive form.[40]

Modulating the Driving Force for Electron Transfer. One possible explanation for the failure to observe a radical spectrum in $dAppA_{BLUF}$, BlsA and BlrB is that the rate of charge separation is small, and that of charge recombination is large, such that no radical population builds up. Charge separation as the rate-determining step would also be consistent with the identical kinetics observed for excited state decay and ground state recovery (Figure 2C, Table 1). To probe this possibility the Tyr21 residue in $dAppA_{BLUF}$ was replaced with two unnatural amino acids, tyrosine fluorinated at positions 2 and 3 (labeled 2FY21 and 3FY21, respectively). This substitution is expected to give a minimum perturbation to the structure, leaving the surrounding residues unchanged.[58,60] However, it will have the effect of modulating the free energy driving the electron transfer reaction, ΔG_0, due to the different redox potential of the three tyrosines. This will modify the rate-determining charge separation step even in the case of slow charge separation and fast recombination. The other factor which will be altered by the Tyr/FTyr exchange is the H-bonding environment, through the pK_a of the acidic proton. These parameters are listed in Table 2, where the formal

Table 2. Thermodynamic Parameters for Fluorinated Tyrosines[a]

A	Tyr	2FTyr	3FTyr	Trp
pK_a	10	9.0	8.4	na
$E(A/A^{\bullet+})$/V	1.34	1.26	1.27	1.07
ΔG_{CS}/eV[b]	−0.83	−0.91	−0.90	−1.1
ΔG_{CR}/eV	−1.67	−1.59	−1.6	−1.4

[a]The redox potentials were measured at pH 7 (protonated form, data shown in Figure S7 in SI) but converted to standard (pH 1), assuming a reversible system. [b]The free energies were calculated according to eqs 2) and (3 assuming $E(F/F^{\bullet-})$ = −0.33 V and 2.5 eV for ΔE S_1 the onset of the $S_0 \rightarrow S_1$ transition and the unknown electrostatic factor has been assumed negligible.

potentials for the fluorinated tyrosine electron donors at physiological pH are reported for the first time. As can be seen, the effect of fluorine substitution alters the potential, but the position of the fluorine substituent has no significant effect.

The locations and shape of the TRIR spectra for the 2FY21 and 3FY21 are very similar to those for $dAppA_{BLUF}$ (SI, Figure S7). This is consistent with a minimal perturbation to the H-bond environment around the flavin ring on exchange for the native Tyr. However, there is a distinct effect on the kinetics with both relaxation times recovered from the biexponential analysis becoming significantly longer for the FTyr proteins (Table 3). However, as was observed for $dAppA_{BLUF}$, there is

Table 3. Excited State Decay and Ground State Recovery Kinetics at the Two Characteristic Frequencies for FTyr Substituted AppA[a]

	frequency/cm^{-1}	Wt τ_1	τ_1/ps	τ_2/ps
2FY21AppA	1380	0.27	118 ± 60	>1000
	1548	0.44	140 ± 80	>1000
3FY21AppA	1380	0.33	50 ± 50	498 ± 300
	1548	0.32	70 ± 33	600 ± 140
dAppA	1380	0.38	17 ± 8	401 ± 110
	1548	0.42	29 ± 5	512 ± 60

[a]Kinetics were fit to a sum of two exponential terms. The data for $dAppA_{BLUF}$ (Table 1) are included for comparison.

no difference between the excited state decay and ground state recovery kinetics, again requiring no significant population of an intermediate state.

For the analysis of these data we turn to the classical Marcus expression for the rate constant of an electron transfer reaction:[68]

dx.doi.org/10.1021/ja4121082 | J. Am. Chem. Soc. 2014, 136, 4605−4615

$$k_{et} = \frac{2\pi\langle V_{el}\rangle^2}{\hbar(4\pi\lambda kT)^{1/2}} \exp -\left[\frac{(\Delta G_0 + \lambda)^2}{4\lambda kT}\right] \quad (1)$$

In 1 V_{el} is the electronic coupling parameter between donor and acceptor and, λ, the reorganization energy, both of which depend in quite complex ways on the details of the local structure and environment, while λ is also a function of the redox potentials.[69−71] The other parameters have their usual meaning. This equation defines the Marcus curve, a parabola with maximum at $-\Delta G_0 = \lambda$ separating the normal and Marcus

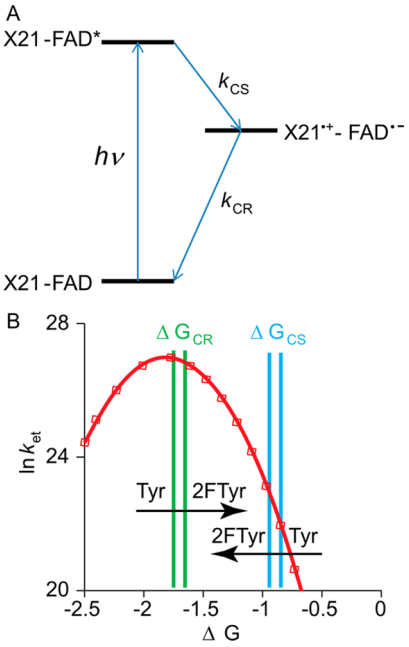

Figure 8. Electron transfer processes in $dAppA_{BLUF}$ and 2/3FY21 mutants. (A) Energy level scheme for charge separation and recombination. (B) Representation of the Marcus equation with λ set to 1.8 eV such that the maximum value for the rate constant is set to match the fastest observed decay time of 2 ps (in Y8W). The ΔG_0 for charge separation and recombination are marked for $dAppA_{BLUF}$ and 2FY21. As ΔG_0 becomes more negative in the normal region, the charge separation rate constant is expected to increase.

inverted regions (Figure 8). The driving force for the forward electron transfer (charge separation, CS) reaction is given by:[70]

$$\Delta G_0(\mathrm{CS}) = E(Y^{+\bullet}/Y) - E(F^{-*}/F) - E_{S1} - \Delta G_\varepsilon \quad (2)$$

the $E(i)$ are the redox potentials of the respective couples, i, E_{S1} the 0−0 energy (in eV)of the electronic transition in FAD and ΔG_ε an electrostatic term, typically less than 0.1 eV. The corresponding expression for charge recombination (CR) is

$$\Delta G_0(\mathrm{CR}) = -E(Y^{+\bullet}/Y) + E(F^{-*}/F) + \Delta G_\varepsilon \quad (3)$$

Thus, by varying the redox potential of the tyrosine the ΔG_0 for CR and CS steps will be modified (Figure 8A); the calculated ΔG_0 are given in Table 2, where the corresponding data for Trp are included for reference to theY21W data.

These data may be compared with the sequential scheme which adequately fits all data sets, where

$$X21 - \mathrm{FAD}^* \xrightarrow{k_{CS}} X21^{\bullet+} - \mathrm{FAD}^{\bullet-} \xrightarrow{k_{CR}} X21 - \mathrm{FAD}$$

X is W or Y and the rate coefficients are now identified with electron transfer. For this scheme the decay of the FAD excited state will be faster than the recovery of the ground state if $k_{CS} > k_{CR}$. This is indeed the case whenever the radical intermediates are observed (Y21W, PixD, Y8W), as shown by the kinetics associated with their respective marker modes in Table 1, Figures 3C, and 6B. However, for $dAppA_{BLUF}$, BlsA, and the two FTyr mutants, the excited state decay and ground state recovery kinetics overlap. This can only happen in the case that $k_{CS} < k_{CR}$, in which case the slow decay of FAD* by electron transfer determines the rate of ground state recovery, and the population of the intermediate will be negligible. For this to be the case requires k_{CS} to decrease substantially between for example PixD and $dAppA_{BLUF}$, with little change or an acceleration in k_{CR}; this would indicate high sensitivity of electron transfer in the BLUF domain to the structure around the flavin ring.

In all cases the driving force for charge recombination is greater than for charge separation (Table 2). In that case, $k_{CS} < k_{CR}$ requires that the electron transfer is in the normal rather than the Marcus inverted region (Figure 8). However, a consequence of being in the normal region is that an increase in driving force, such as is observed when Tyr is exchanged for FTyr, is predicted to result in an increased rate of charge separation (Figure 8B). What is in fact observed is a decrease in that rate (a longer excited state decay, Table 3). Thus, the changes in kinetics observed when FTyr replaces Tyr21 in $dAppA_{BLUF}$ are not consistent with a simple excited state electron transfer quenching mechanism. This observation is consistent with the lack of any measurable population of radical intermediate states (Figure 2A). This conclusion applies also to BlsA and (on the basis of the optical spectroscopy[44]) BlrB, but not to PixD, where a radical intermediate is clearly observed, as already reported.[38,43] Significantly, fluorotyrosine substitution was also used in PixD, and an increase in the excited state decay time was also reported, although the redox potentials were not available at that time.[43] The most straightforward interpretation of these data is that in AppA (and by extension BlsA and BlrB) charge separation to form a radical intermediate is not the primary step in the BLUF domain photocycle. This is a conclusion which has important implications for theoretical modeling of the BLUF domain. Further, the conclusion does not depend on the choice of λ, which has the effect of shifting the Marcus curve, and therefore the inverted region, to smaller ΔG for a smaller λ; this increases k_{CS}, but does not alter the effect of making ΔG more negative (Table 2), which is a predicted acceleration in k_{CS}. This is true until k_{CS} falls within the inverted region (for $\lambda < 0.9$ eV), but in that case $k_{CS} > k_{CR}$, which is not observed. Thus, the fluorotyrosine data support the conclusion that at least $k_{CR} \gg k_{CS}$, and any radical state must have only a fleeting existence and not act as a metastable intermediate about which structural reorganization occurs.

The observation of electron transfer reactions in PixD (and in Y21W and Y8W) may arise because the driving forces are quite different from those in Table 1, indicative of specific medium effects on the redox potentials and the relative geometry of donor and acceptor (which will modify V_{el}). Such changes could have the effect of placing the charge recombination in the inverted region, decreasing the rate of charge recombination, allowing observation of the intermediate (Figure 8B). Such effects on electron transfer reactions in protein are intrinsically interesting but not obviously associated with BLUF domain function.

dx.doi.org/10.1021/ja4121082 | J. Am. Chem. Soc. 2014, 136, 4605−4615

A Nonradical Intermediate Pathway for the Primary Step in BLUF Domain Proteins. In the absence of unambiguous experimental evidence for radical intermediates in the primary photochemistry of $dAppA_{BLUF}$ (and at least two other BLUF proteins), it is necessary to propose an alternative pathway to the altered H-bond structure and red-shifted absorption known to be associated with photoactive BLUF domains. Both we and Domratcheva and co-workers previously considered the possibility of photoinduced tautomerization being sufficient to modify the structure of the key residue Q63.[29,48] In our model the electronic ground state supports equilibrium between the dominant keto and minor enol forms of Q63.[48,49] The present kinetic and spectroscopic data (Figure 2) and recent calculations[33] suggest that a distribution of ground state structures exists, which may correspond with a distribution in the position of the keto−enol equilibrium. Upon electronic excitation of the flavin ring, the strength of the H-bonds formed between it and the surrounding amino acid residues (Y21, Q63, N45, W104) may be modified by changes in electron density in the flavin ring. It is proposed that this is sufficient to drive the position of the equilibrium to the enol form. The resulting rearrangement in the H-bond environment in the excited state occurs on a subpicosecond time scale. Ultrafast changes in the environment of the chromophore consistent with an excitation-induced change in H-bond structure have been observed in TRIR measurements and may be consistent with the tautomerization (Figure 2 and S1).[48,49] In the future TRIR measurements on isotope-labeled AppA will be undertaken to test this assignment, targeting Q63 and other residues involved in the H-bond structure around the flavin (Figure 1). Electronic relaxation of the reorganized structure back to the ground state leaves the flavin in an altered H-bond environment, one which is not directly accessible from the dark ground electronic state. This unstable form of the ground state can either relax back to the original ground state (the dominant pathway judged from the kinetic data) or populate the red-shifted state, for example through isomerization of the enol form of Q63 and subsequent H-bond reorganization.

Although no radical intermediates were detected for $dAppA_{BLUF}$ or BlsA, and modulation of the driving force for electron transfer did not support a charge separation reaction, we cannot absolutely rule out a role for the electron transfer reaction coordinate. It is plausible that motion along the reactive coordinate leading to electron transfer results in excited state quenching, with the ultrafast charge recombination placing the BLUF domain in the unstable neutral ground state configuration, as proposed above. The precise pathway for the reorganization of this configuration may be revealed by the kind of QM/MM calculations that have begun to appear.[26−29,33,52,54] However, such calculations must be informed by the knowledge that radical intermediate states are, at most, a fleeting entity; thus, alternative pathways should be considered.

CONCLUSION

The primary processes in the BLUF domain have been investigated by ultrafast TRIR spectroscopy. Marker modes were identified for the flavin excited and ground electronic states and for the flavin radical anion. High signal-to-noise 100 fs time resolution studies of the transient spectra and kinetics of $dAppA_{BLUF}$ did not reveal the formation of any new states which could be assigned to a radical (or any other) intermediate. Radical intermediates were however readily observed in the photoinactive Y21W mutant of $dAppA_{BLUF}$, and the kinetics of the photoinduced electron transfer were characterized. Radical intermediates have subsequently been observed in a number of other photoinactive states of $AppA_{BLUF}$ (unpublished data), but there is no correlation between the observation of photoactivity and formation of a significant population of radical intermediates. The possibility that the population of radical intermediates was kinetically limited was tested by assuming that electron transfer does occur and modifying the thermodynamic driving force through unnatural amino acid substitution. Those data were also not consistent with photoinduced electron transfer being the primary process in $dAppA_{BLUF}$. Thus, the present data for $dAppA_{BLUF}$ are in contradiction to the widely accepted mechanism for BLUF domain function, photoinduced electron transfer between Tyr21 and FAD* leading to a radical intermediate.

The TRIR measurements were extended to the BLUF domain proteins PixD and BlsA. Radical formation was observed in PixD in good agreement with earlier observations.[45] However, no radical intermediates were found in BlsA, and a similar null result was recently reported in a fourth BLUF domain, BlrB.[51] These data suggest that the Y21-to-flavin electron transfer is a sensitive function of BLUF domain structure. However, although electron transfer intermediates are observed in PixD and in other photoinactive mutants of $dAppA_{BLUF}$ (and in its light-adapted form, unpublished data) there is no correlation between the rate of electron transfer and photoactivity. Consequently we considered alternative pathways to signaling state formation in the BLUF domain. It was proposed that electronic excitation is itself sufficient to induce H-bond reorganization in the flavin environment. This could arise through the modified electronic structure of the flavin excited state. There is existing experimental evidence for such a coupling between electronic excitation and changes in protein structure.[49] It was suggested that this change in H-bonding is sufficient to perturb the position of keto−enol tautomerization in the key Q63 residue,[29,48] and that this is the primary event which leads to the subsequent structural reorganization and ultimately to formation of the signaling state.

ASSOCIATED CONTENT

Supporting Information

Further experimental methods along with additional TRIR spectra and electrochemistry data. This material is available free of charge via the Internet at http://pubs.acs.org.

AUTHOR INFORMATION

Corresponding Authors

(P.J.T.) peter.tonge@stonybrook.edu
(S.R.M.) s.meech@uea.ac.uk

Present Addresses

[⊥]The Scripps Research Institute, 130 Scripps Way, Jupiter, FL 33458, United States.
[†]The Wistar Institute, Philadelphia, PA 19104, United States.

Notes

The authors declare no competing financial interest.

ACKNOWLEDGMENTS

Funded by EPSRC (EP/K000764/1) to S.R.M.), STFC (Program 101005 to S.R.M. and P.J.T.) and NSF (CHE-

1223819 to P.J.T.).The authors are grateful to STFC for access to the Central Laser Facility. We are also grateful to the Oxford Protein Production Facility (OPPF) for their assistance in sample preparation. K.A. thanks UEA for the award of a studentship. A.L. was supported by the European Union and the State of Hungary, co-financed by the European Social Fund in the framework of TAMOP-4.2.4.A/2-11/1-2012-0001 'National Excellence Program.' We are grateful to Dr. Gregory G. Wildgoose (UEA) for the determination of the formal potentials.

REFERENCES

(1) Moglich, A.; Yang, X. J.; Ayers, R. A.; Moffat, K. *Annu. Rev. Plant Biol.* **2010**, *61*, 21.
(2) Van der Horst, M. A.; Hellingwerf, K. J. *Acc. Chem. Res.* **2004**, *37*, 13.
(3) Losi, A. *Photochem. Photobiol.* **2007**, *83*, 1283.
(4) Losi, A.; Gartner, W. *Photochem. Photobiol.* **2010**, *87*, 491.
(5) Braatsch, S.; Klug, G. *Photosynth. Res.* **2004**, *79*, 45.
(6) Masuda, S. *Plant Cell Physiol.* **2013**, *54*, 171.
(7) Kennis, J. T. M.; Groot, M. L. *Curr. Opin. Struct. Biol.* **2007**, *17*, 623.
(8) Lukacs, A.; Eker, A. P. M.; Byrdin, M.; Brettel, K.; Vos, M. H. In *Ultrafast Phenomena XVI: Proceedings of the 16th International Conference, Palazzo dei Congressi Stresa, Italy, June 9−13, 2008*; Corkum, P., DeSilvestri, S., Nelson, K. A., Riedle, E., ; Schoenlein, R. W., Eds.; Springer Series in Chemical Physics, Vol. *92*, **2009**; p 604.
(9) Lukacs, A.; Eker, A. P. M.; Byrdin, M.; Villette, S.; Pan, J.; Brettel, K.; Vos, M. H. *J. Phys. Chem. B* **2006**, *110*, 15654.
(10) Sato, Y.; Iwata, T.; Tokutomi, S.; Kandori, H. *J. Am. Chem. Soc.* **2005**, *127*, 1088.
(11) Kottke, T.; Heberle, J.; Hehn, D.; Dick, B.; Hegemann, P. *Biophys. J.* **2003**, *84*, 1192.
(12) Okajima, K.; Yoshihara, S.; Fukushima, Y.; Geng, X. X.; Katayama, M.; Higashi, S.; Watanabe, M.; Sato, S.; Tabata, S.; Shibata, Y.; Itoh, S.; Ikeuchi, M. *J. Biochem.* **2005**, *137*, 741.
(13) Fiedler, B.; Borner, T.; Wilde, A. *Photochem. Photobiol.* **2005**, *81*, 1481.
(14) Mussi, M. A.; Gaddy, J. A.; Cabruja, M.; Arivett, B. A.; Viale, A. M.; Rasia, R.; Actis, L. A. *J. Bacteriol.* **2010**, *192*, 6336.
(15) Gomelsky, M.; Klug, G. *Trends Biochem. Sci.* **2002**, *27*, 497.
(16) Laan, W.; van der Horst, M. A.; van Stokkum, I. H.; Hellingwerf, K. J. *Photochem. Photobiol.* **2003**, *78*, 290.
(17) Stierl, M.; Stumpf, P.; Udwari, D.; Gueta, R.; Hagedorn, R.; Losi, A.; Gartner, W.; Petereit, L.; Efetova, M.; Schwarzel, M.; Oertner, T. G.; Nagel, G.; Hegemann, P. *J. Biol. Chem.* **2011**, *286*, 1181.
(18) Pimenta, F. M.; Jensen, R. L.; Breitenbach, T.; Etzerodt, M.; Ogilby, P. R. *Photochem. Photobiol.* **2013**, *89*, 1116.
(19) Ruiz-Gonzalez, R.; Cortajarena, A. L.; Mejias, S. H.; Agut, M.; Nonell, S.; Flors, C. *J. Am. Chem. Soc.* **2013**, *135*, 9564.
(20) Masuda, S.; Hasegawa, K.; Ishii, A.; Ono, T. *Biochemistry* **2004**, *43*, 5304.
(21) Masuda, S.; Hasegawa, K.; Ono, T. *Biochemistry* **2005**, *44*, 1215.
(22) Anderson, S.; Dragnea, V.; Masuda, S.; Ybe, J.; Moffat, K.; Bauer, C. *Biochemistry* **2005**, *44*, 7998.
(23) Jung, A.; Domratcheva, T.; Tarutina, M.; Wu, Q.; Ko, W. H.; Shoeman, R. L.; Gomelsky, M.; Gardner, K. H.; Schlichting, L. *Proc. Natl. Acad. Sci. U.S.A.* **2005**, *102*, 12350.
(24) Masuda, S.; Bauer, C. E. *Cell* **2002**, *110*, 613.
(25) Grinstead, J. S.; Hsu, S. T. D.; Laan, W.; Bonvin, A.; Hellingwerf, K. J.; Boelens, R.; Kaptein, R. *ChemBioChem* **2006**, *7*, 187.
(26) Hsiao, Y.-W.; Goetze, J. P.; Thiel, W. *J. Phys. Chem. B* **2012**, *116*, 8064.
(27) Sadeghian, K.; Bocola, M.; Schuetz, M. *J. Am. Chem. Soc.* **2008**, *130*, 12501.
(28) Sadeghian, K.; Bocola, M.; Schuetz, M. *Phys. Chem. Chem. Phys.* **2010**, *12*, 8840.
(29) Domratcheva, T.; Grigorenko, B. L.; Schlichting, I.; Nemukhin, A. V. *Biophys. J.* **2008**, *94*, 3872.
(30) Meier, K.; van Gunsteren, W. F. *Mol. Simulat.* **2013**, *39*, 472.
(31) Meier, K.; Thiel, W.; van Gunsteren, W. F. *J. Comput. Chem.* **2012**, *33*, 363.
(32) Sadeghian, K.; Bocola, M.; Schutz, M. *J. Am. Chem. Soc.* **2008**, *130*, 12501.
(33) Udvarhelyi, A.; Domratcheva, T. *J. Phys. Chem. B* **2013**, *117*, 2888.
(34) Unno, M.; Masuda, S.; Ono, T. A.; Yamauchi, S. *J. Am. Chem. Soc.* **2006**, *128*, 5638.
(35) Unno, M.; Sano, R.; Masuda, S.; Ono, T. A.; Yamauchi, S. *J. Phys. Chem. B* **2005**, *109*, 12620.
(36) *The Pymol Molecular Graphics System*, version 1.5.0.5; Schrödinger, LLC., New York, 2013.
(37) Masuda, S.; Tomida, Y.; Ohta, H.; Takamiya, K. I. *J. Mol. Biol.* **2007**, *368*, 1223.
(38) Bonetti, C.; Stierl, M.; Mathes, T.; van Stokkum, I. H. M.; Mullen, K. M.; Cohen-Stuart, T. A.; van Grondelle, R.; Hegemann, P.; Kennis, J. T. M. *Biochemistry* **2009**, *48*, 11458.
(39) Dragnea, V.; Arunkumar, A. I.; Yuan, H.; Giedroc, D. P.; Bauer, C. E. *Biochemistry* **2009**, *48*, 9969.
(40) Brust, R.; Lukacs, A.; Haigney, A.; Addison, K.; Gil, A.; Towrie, M.; Clark, I. P.; Greetham, G. M.; Tonge, P. J.; Meech, S. R. *J. Am. Chem. Soc.* **2013**, *135*, 16168.
(41) Gauden, M.; Grinstead, J. S.; Laan, W.; van Stokkum, I. H. M.; Avila-Perez, M.; Toh, K. C.; Boelens, R.; Kaptein, R.; van Grondelle, R.; Hellingwerf, K. J.; Kennis, J. T. M. *Biochemistry* **2007**, *46*, 7405.
(42) Laan, W.; Gauden, M.; Yeremenko, S.; van Grondelle, R.; Kennis, J. T. M.; Hellingwerf, K. J. *Biochemistry* **2006**, *45*, 51.
(43) Mathes, T.; van Stokkum, I. H. M.; Stierl, M.; Kennis, J. T. M. *J. Biol. Chem.* **2012**, *287*, 31725.
(44) Mathes, T.; Zhu, J. Y.; van Stokkum, I. H. M.; Groot, M. L.; Hegemann, P.; Kennis, J. T. M. *J. Phys. Chem. Lett.* **2012**, *3*, 203.
(45) Gauden, M.; van Stokkum, I. H. M.; Key, J. M.; Luhrs, D. C.; Van Grondelle, R.; Hegemann, P.; Kennis, J. T. M. *Proc. Natl. Acad. Sci. U.S.A.* **2006**, *103*, 10895.
(46) Bonetti, C.; Mathes, T.; van Stokkum, I. H. M.; Mullen, K. M.; Groot, M. L.; van Grondelle, R.; Hegemann, P.; Kennis, J. T. M. *Biophys. J.* **2008**, *95*, 4790.
(47) Gauden, M.; Yeremenko, S.; Laan, W.; van Stokkum, I. H. M.; Ihalainen, J. A.; van Grondelle, R.; Hellingwerf, K. J.; Kennis, J. T. M. *Biochemistry* **2005**, *44*, 3653.
(48) Stelling, A. L.; Ronayne, K. L.; Nappa, J.; Tonge, P. J.; Meech, S. R. *J. Am. Chem. Soc.* **2007**, *129*, 15556.
(49) Lukacs, A.; Haigney, A.; Brust, R.; Zhao, R. K.; Stelling, A. L.; Clark, I. P.; Towrie, M.; Greetham, G. M.; Meech, S. R.; Tonge, P. J. *J. Am. Chem. Soc.* **2011**, *133*, 16893.
(50) Brust, R.; Haigney, A.; Lukacs, A.; Gil, A.; Hossain, S.; Addison, K.; Lai, C.-T.; Towrie, M.; Greetham, G. M.; Clark, I. P.; Illarionov, B.; Bacher, A.; Kim, R.-R.; Fischer, M.; Simmerling, C.; Meech, S. R.; Tonge, P. J. *J. Phys. Chem. Lett.* **2013**, *5*, 220.
(51) Mathes, T.; van Stokkum, I. H. M.; Bonetti, C.; Hegemann, P.; Kennis, J. T. M. *J. Phys. Chem. B* **2011**, *115*, 7963.
(52) Khrenova, M. G.; Nemukhin, A. V.; Grigorenko, B. L.; Krylov, A. I.; Domratcheva, T. M. *J. Chem. Theory Comput.* **2010**, *6*, 2293.
(53) Udvarhelyi, A.; Domratcheva, T. *Photochem. Photobiol.* **2011**, *87*, 554.
(54) Khrenova, M. G.; Nemukhin, A. V.; Domratcheva, T. *J. Phys. Chem. B* **2013**, *117*, 2369.
(55) Haigney, A.; Lukacs, A.; Brust, R.; Zhao, R. K.; Towrie, M.; Greetham, G. M.; Clark, I.; Illarionov, B.; Bacher, A.; Kim, R. R.; Fischer, M.; Meech, S. R.; Tonge, P. J. *J. Phys. Chem. B* **2012**, *116*, 10722.
(56) Haigney, A.; Lukacs, A.; Zhao, R. K.; Stelling, A. L.; Brust, R.; Kim, R. R.; Kondo, M.; Clark, I.; Towrie, M.; Greetham, G. M.; Illarionov, B.; Bacher, A.; Romisch-Margl, W.; Fischer, M.; Meech, S. R.; Tonge, P. J. *Biochemistry* **2011**, *50*, 1321.

(57) Zhao, R.-K.; Lukacs, A.; Haigney, A.; Brust, R.; Greetham, G. M.; Towrie, M.; Tonge, P. J.; Meech, S. R. *Phys. Chem. Chem. Phys.* **2011**, *13*, 17642.
(58) Reece, S. Y.; Seyedsayamdost, M. R.; Stubbe, J.; Nocera, D. G. *J. Am. Chem. Soc.* **2007**, *129*, 13828.
(59) Greetham, G. M.; Burgos, P.; Cao, Q. A.; Clark, I. P.; Codd, P. S.; Farrow, R. C.; George, M. W.; Kogimtzis, M.; Matousek, P.; Parker, A. W.; Pollard, M. R.; Robinson, D. A.; Xin, Z. J.; Towrie, M. *Appl. Spectrosc.* **2011**, *64*, 1311.
(60) Reece, S. Y.; Seyedsayamdost, M. R.; Stubbe, J.; Nocera, D. G. *J. Am. Chem. Soc.* **2006**, *128*, 13654.
(61) Seyedsayamdost, M. R.; Reece, S. Y.; Nocera, D. G.; Stubbe, J. *J. Am. Chem. Soc.* **2006**, *128*, 1569.
(62) Tommos, C.; Skalicky, J. J.; Pilloud, D. L.; Wand, A. J.; Dutton, P. L. *Biochemistry* **1999**, *38*, 9495.
(63) Kondo, M.; Nappa, J.; Ronayne, K. L.; Stelling, A. L.; Tonge, P. J.; Meech, S. R. *J. Phys. Chem. B* **2006**, *110*, 20107.
(64) Lukacs, A.; Zhao, R. K.; Haigney, A.; Brust, R.; Greetham, G. M.; Towrie, M.; Tonge, P. J.; Meech, S. R. *J. Phys. Chem. B* **2012**, *116*, 5810.
(65) Wolf, M. M. N.; Schumann, C.; Gross, R.; Domratcheva, T.; Diller, R. *J. Phys. Chem. B* **2008**, *112*, 13424.
(66) Ishikita, H. *J. Biol. Chem.* **2008**, *283*, 30618.
(67) Walden, S. E.; Wheeler, R. A. *J. Chem. Soc., Perkin Trans. 2* **1996**, 2663.
(68) Marcus, R. A.; Sutin, N. *Biochim. Biophys. Acta* **1985**, *811*, 265.
(69) Duvanel, G.; Grilj, J.; Vauthey, E. *J. Phys. Chem. A* **2013**, *117*, 918.
(70) Rosspeintner, A.; Angulo, G.; Vauthey, E. *J. Phys. Chem. A* **2012**, *116*, 9473.
(71) Rosspeintner, A.; Lang, B.; Vauthey, E. In *Annu. Rev. Phys. Chem.*; Johnson, M. A., Martinez, T. J., Eds. **2013**; Vol. *64*, p 247.